

Analysis of Parenchymal Texture Properties in Breast Tomosynthesis Images

Despina Kontos*, Predrag R. Bakic and Andrew D.A. Maidment
University of Pennsylvania, Department of Radiology, 3400 Spruce St., Philadelphia PA 19104
{Despina.Kontos | Predrag.Bakic | Andrew.Maidment} @uphs.upenn.edu

ABSTRACT

We have analyzed breast parenchymal texture in tomosynthesis images. Tomosynthesis is a novel x-ray imaging modality in which 3D images of the breast are reconstructed from multiple 2D x-ray source projection images acquired by varying the angle of the x-ray tube. Our ultimate goal is to examine the correlation between tomosynthesis texture descriptors and breast cancer risk. As a first step, we investigated the effect of tomosynthesis acquisition parameters on texture in the source projection images; this avoids the influence of the reconstruction algorithm. We computed statistical texture descriptors which have been shown in the literature to be highly indicative of breast cancer risk. We compared skewness, coarseness, and contrast computed from the central source projection images and the corresponding mammograms. Our analysis showed that differences exist between mammographic and tomosynthetic texture in projection images. Retroareolar ROIs in tomosynthesis images appeared to be less skewed with lower coarseness and higher contrast measures compared to mammograms; however, corresponding texture descriptors for tomosynthesis and mammography are correlated. Examination of the ROIs demonstrates that the texture in tomosynthesis source projections visually differs from the x-ray mammograms. We attribute this observation to acquisition differences, including radiation dose, compression force, and x-ray scatter. As with mammography, tomosynthesis parenchymal texture is related to the Gail-model cancer risk. Although preliminary, we believe that texture analysis of 3D breast tomosynthesis images will ultimately yield more accurate and precise measures of risk.

Keywords: Effect of physical imaging parameters, Quantitative image analysis, Parenchymal texture, Feature extraction, Digital breast tomosynthesis, Mammography, Breast cancer risk assessment

1. INTRODUCTION

Several studies have shown a relationship between mammographic parenchymal patterns and the risk of developing breast cancer (1, 2). Parenchymal patterns are the mammographic visual effect of breast density, which has been identified as one of the major biomarkers of cancer risk; being indicative of changes in risk factors such as hormonal levels, diet and body mass index (3, 4). Breast parenchyma, as visualized mammographically, has been analyzed in terms of texture for the purpose of breast cancer risk assessment (2); image-based texture features computed from the retroareolar breast region have been shown to be indicative in distinguishing between different risk groups of women (5-7). Quantitative methods for estimating breast density, based on gray-level pixel values, have been developed to measure the breast density from digitized 2D x-ray mammograms and estimate the relative breast cancer risk (8).

The analysis of parenchymal patterns in breast images provides the foundation for establishing robust image-based descriptors that can be used to improve cancer risk estimation. However, current projection mammography imposes restrictions for accurately quantifying breast parenchymal properties; 2D mammograms do not allow for visual separation of the 3D fibroglandular tissue. Consequently, accurate volumetric assessment of glandular tissue properties based on image texture is not possible; 2D texture descriptors do not accurately reflect the actual 3D breast parenchyma. As it is likely that cancer risk is related to the actual volumetric distribution (9) and amount of glandular tissue rather than the projected 2D area, 3D imaging of the breast could provide more realistic means for parenchymal analysis.

* Despina.Kontos@uphs.upenn.edu; phone 1 215 746 8759; fax 1 215 746 8764

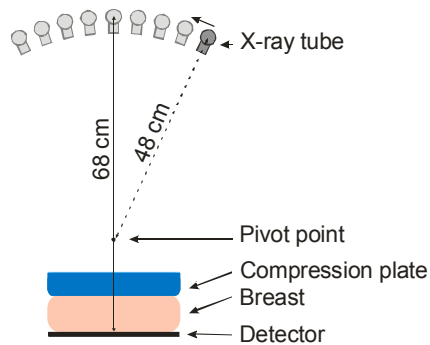


Fig. 1. X-ray acquisition geometry for digital breast tomosynthesis.

Digital breast tomosynthesis (DBT) is a novel 3D x-ray imaging technique in which tomographic images of the breast are reconstructed from multiple low-dose 2D x-ray projection images (10). The projections are acquired by varying the position of the x-ray focus (see Figure 1). By combining information from different projections, the distribution of parenchymal tissue is accurately visualized in 3D and superimposition is avoided. For this reason more accurate quantitative analysis of the breast parenchyma is possible. Compared to mammography, DBT provides superior tissue visualization and lesion identification (11). The improved performance and low cost of breast tomosynthesis will likely fuel the rapid and broad dissemination of tomosynthesis as a breast cancer screening modality.

In this work we perform analysis of breast parenchymal texture properties in tomosynthesis images. Our ultimate goal is to investigate the relationship between breast cancer risk and parenchymal patterns as visualized by breast tomosynthesis. As a first step towards this goal, we have investigated the effect of tomosynthesis acquisition parameters on texture in the tomosynthesis source projection images. This analysis is independent of reconstruction algorithm (12) and provides a baseline for comparing texture initially with 2D mammograms and ultimately with fully 3D texture assessment from reconstructed tomosynthesis images.

We computed statistical texture descriptors which have been shown in the literature to be highly indicative of breast cancer risk (5, 13). We studied the effect of dose, projection angle, compression and scattered radiation during tomosynthesis acquisition on specific texture features. We compared the values of texture features computed from the central source projection (CSP) images and the corresponding mammograms. The CSP is the tomosynthetic source image acquired normal to the detector; it is equivalent to a low-dose mammogram (see Figure 2). We also studied the variation of the texture features among consecutive source projection angles and between each angle and the CSP image; this analysis provides insight to understanding how texture is affected by tomosynthetic angle variation and which texture descriptors are more sensitive in capturing this effect. Finally, we investigated the effect of scattered radiation on texture in tomosynthesis source projection images by comparing to the corresponding mammographic texture features.

Our long-term hypothesis is that 3D parenchymal analysis of breast tomosynthesis images will yield more accurate and precise measures of risk compared to 2D projection mammography. Texture analysis in tomosynthesis source projection images provides a first step towards understanding how 3D image acquisition parameters, such as angle, dose and scatter, affect the visualization of the breast parenchyma in DBT images compared to mammography. This knowledge is essential for developing robust image-based biomarkers for cancer risk estimation. The potential to eventually improve breast cancer risk estimation based on tomosynthesis breast parenchymal properties can be of great clinical advantage; accurate risk assessment is essential for customizing detection, tailoring individual treatment and forming preventive interventions, especially for women associated with a higher risk of breast cancer.

2. METHODS

2.1 Dataset

We have developed a database of tomosynthesis images, mammograms, and corresponding risk estimates. The images included in our analysis have been retrospectively collected from an ongoing clinical multimodality imaging study in our department (NIH R01 CA85484-01A2). Eligible participants include women at high risk, women with recently detected abnormalities, and follow-up of previous cancer patients. During the same day, the women are imaged with digital mammography, DBT, whole breast ultrasound, MRI, PET, and optical imaging. Following informed consent, the women are interviewed in order to calculate their breast cancer risk using the Gail and Claus models (14, 15). The individual imaging results are reviewed in a consensus meeting of expert radiologists. The DBT projections are acquired on a GE Senographe 2000D (General Electric Medical Systems, Milwaukee, WI), modified to allow the x-ray tube to be positioned at 9 locations by varying the angle from -25° to $+25^\circ$ with increments of 6.25° (see Figure 2). The breast is compressed in an MLO position and the source images are acquired with spatial resolution of 100 microns/pixel.



Fig. 2. An example of tomosynthetic acquisition with 9 source projection images, each 6.25 degrees apart. The 0° degree angle corresponds to the central source projection (CSP) image.

To date, 52 women have had breast tomosynthesis images and mammograms as part of this NIH study. For our parenchymal pattern analysis we excluded women with unilateral imaging, incomplete data and significant visual image artifacts; bilateral tomosynthesis images and mammograms from 40 women were included in our texture analysis (mean age 51.4 years, range 31-80). The average lifetime Gail risk value for these 40 women was 10.78%. These images, along with the clinical information available for these women (pathology, likelihood of malignancy, BIRADS, etc.) and the risk estimates from Claus and Gail models, have been stored in an RSNA MIRC database (16) that we have customized. All the data stored in the MIRC database have been anonymized using the built-in anonymization tool.

For computing texture descriptors, we have manually selected clinically relevant regions of interest (ROIs); it has been shown that retroareolar ROIs are highly discriminative in distinguishing among women at different cancer risk levels, such as low risk women versus BRCA1/2 gene mutation carriers (7, 13, 17). Retroareolar ROIs of 256x256 pixel size (0.1mm/pixel) were manually segmented from the DBT source projection images and the corresponding mammograms; both imaging modalities were preprocessed with the GE *Premium View*TM algorithm. Examples of such ROIs are shown in Figure 3.

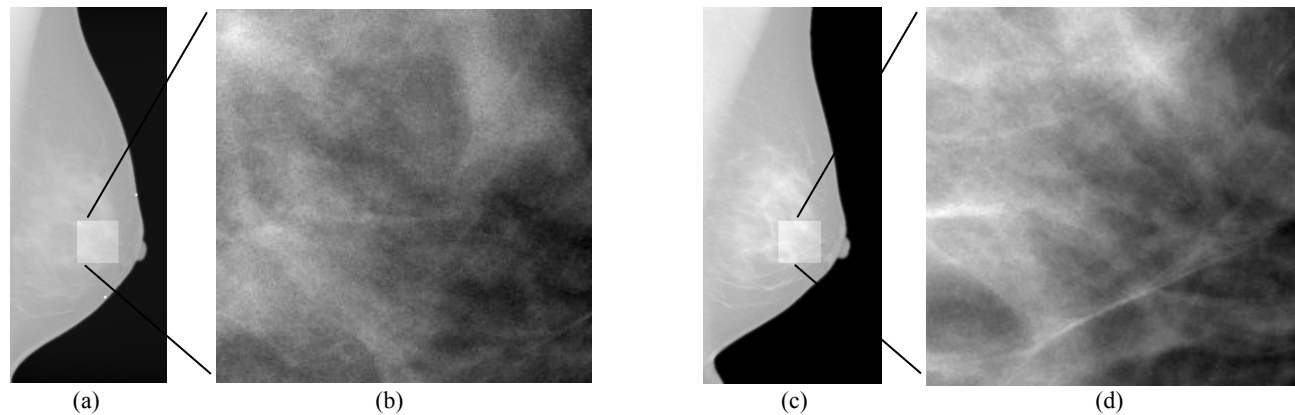


Fig. 3. Example of a retroareolar ROI segmented manually from (a-b) a tomosynthesis central source projection image and (c-d) the corresponding MLO mammogram.

2.2 Texture analysis

We implemented texture descriptors that have been shown in the literature (5-7, 17) to be highly effective both in distinguishing among low-risk and high-risk groups of women and correlating parenchymal texture with breast cancer risk as calculated by the Gail and Claus models (5, 6). We computed skewness, coarseness and contrast from all the available ROIs in tomosynthesis source projection images and the corresponding mammographic ROIs; these texture features have been previously defined elsewhere (5, 6, 18, 19) and are given by the following equations:

Skewness is a texture feature reflecting gray-level histogram properties of the image region; it is a measure of the asymmetry of the pixel value distribution around the mean. When the skewness is negative, the gray-level histogram is spread out more to lower values; when the skewness is positive, the gray-level histogram is spread out more to higher values.

$$skewness = \frac{w_3}{w_2^{3/2}}, \text{ where } w_k = \sum_{i=0}^{g_{\max}} n_i (i - \bar{i})^k / N, \quad N = \sum_{i=0}^{g_{\max}} n_i \text{ and } \bar{i} = \sum_{i=0}^{g_{\max}} (in_i / N)$$

In the above formulas, n_i represents the number of times that gray level value i takes place in the image region, g_{max} is the maximum gray-level value and N is the total number of image pixels.

Skewness has been used in other studies as being indicative of breast density (5); when the image texture is predominantly composed by fat the skewness tends to be positive, whereas when the texture is primarily formed by dense tissue the skewness values are negative.

Coarseness is a texture feature that reflects the local variation in image intensity and is based on the Neighborhood Gray Tone Difference Matrix (NGTDM) (5, 18). The NGTDM is computed from the difference among all gray levels within a neighborhood of pixels and a particular gray level, and the average gray level value of the neighboring pixels.

$$coarseness = \left(\sum_{i=0}^{g_{max}} p_i v(i) \right)^{-1}, \text{ where } v(i) = \begin{cases} \sum |i - \bar{L}_i| & \text{for } i \in \{n_i\} \text{ if } n_i \neq 0 \\ 0 & \text{otherwise} \end{cases} \text{ is the NGTDM}$$

In the above formulas, g_{max} is the maximum gray-level value, p_i is the probability that gray level i occurs, $\{n_i\}$ is the set of pixels having gray level value equal to i , and \bar{L}_i is given by

$$\bar{L}_i = \frac{1}{S-1} \sum_{k=-t}^t \sum_{l=-t}^t j(x+k, y+l),$$

where $j(x,y)$ is the pixel located at (x,y) with gray level value i , $(k,l) \neq (0,0)$ and $S=(2d+1)^2$ with d specifying the neighborhood size around the pixel located at (x,y) . Small coarseness value for an ROI indicates fine texture, where the gray levels of neighboring pixels are different; high coarseness value indicates coarse texture, where neighboring pixels have similar gray level values.

Contrast is a texture feature that reveals information on the spatial relationship among different gray levels in the image region and is based on the co-occurrence matrix of gray level pixel values within the image (5, 19).

$$contrast = \sum_{z=0}^{g-1} z^2 \left\{ \sum_i \sum_j c(i, j) \right\},$$

where $|i-j|=k$, g is the total number of different gray levels and c is the normalized co-occurrence matrix for the gray levels in the image region. The contrast descriptor, as computed based on the gray level co-occurrence matrix, provides a measure of the intensity contrast between a pixel and its adjacent pixel over the entire image.

3. RESULTS AND DISCUSSION

We performed parenchymal pattern analysis to (i) compare tomosynthesis texture with mammographic texture, (ii) examine the variation of texture descriptors over the different projection angles in tomosynthetic acquisition and (iii) investigate the effect of scattered radiation on tomosynthesis texture.

3.1 Comparison of tomosynthetic and mammographic texture

For comparing tomosynthetic to mammographic texture we considered the tomosynthesis central source projection (see Figure 2); this projection is acquired normal to the detector and is equivalent to a low-dose mammogram. We computed skewness, coarseness and contrast from all the retroareolar ROIs in the central source projections and compared these values with the corresponding mammographic ROIs (see Figure 3 for an example of such ROIs); we applied one-tailed paired Students T-test (20) at 0.05 significance level to assess the difference in the mean and we computed the correlation coefficient ρ among the two modalities (20). These results are shown in Figures 4-6.

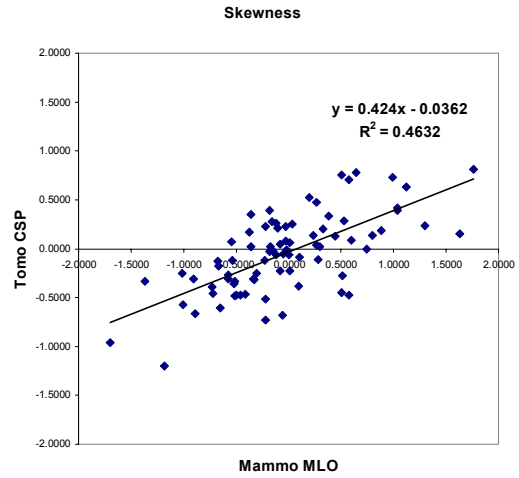
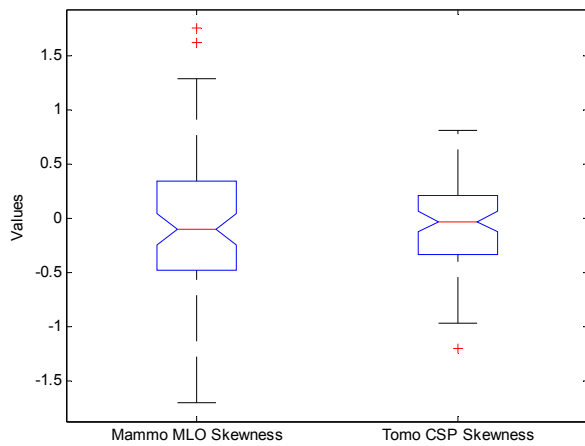


Fig. 4. Skewness values for DBT CSP and MLO mammograms (left) and corresponding scatter-plot (right).

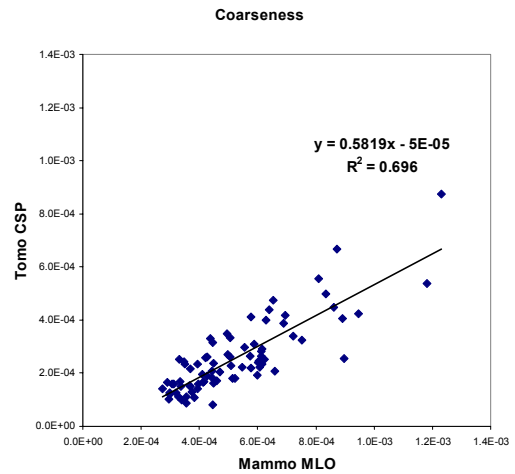
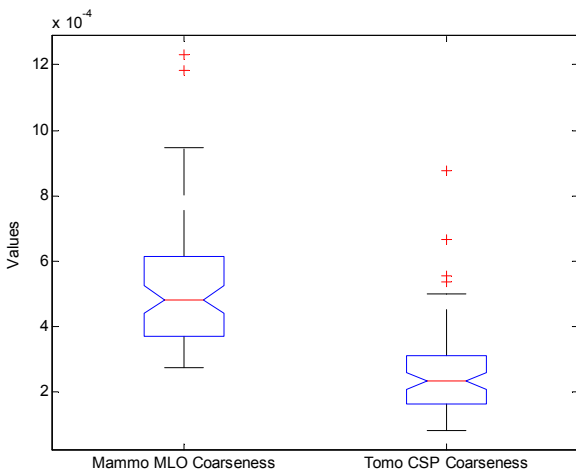


Fig. 5. Coarseness values for DBT CSP and MLO mammograms (left) and corresponding scatter-plot (right).

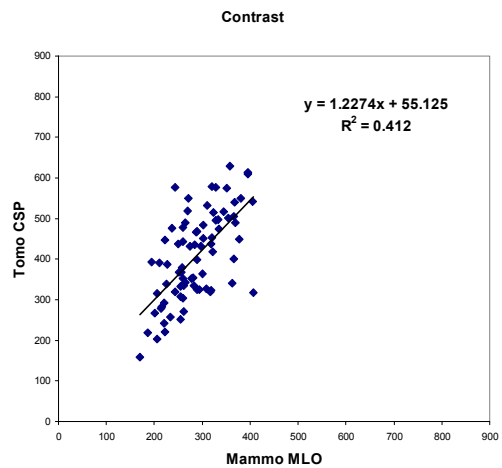
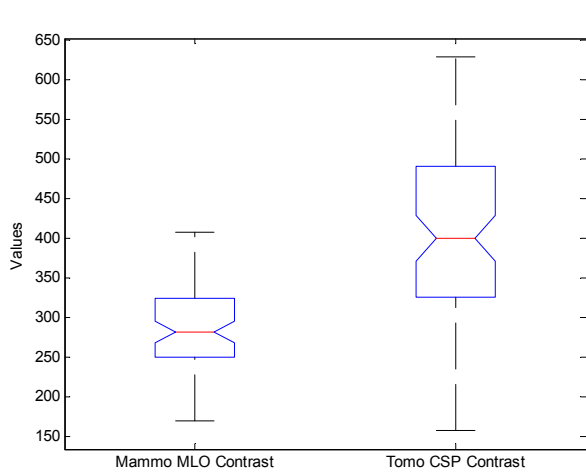


Fig. 6. Contrast values for DBT CSP and MLO mammograms (left) and corresponding scatter-plot (right).

Skewness values in the tomosynthesis images did not appear to be statistically significant different than those in mammograms; the skewness values are correlated for the two modalities ($\rho=0.68$). However, as shown in Figure 4, the range of skewness values in mammograms is approximately twice the range of values in tomosynthesis; in terms of the skewness absolute values, tomosynthesis ROIs appeared to be less skewed compared to mammograms ($p\text{-value}<0.001$). Coarseness values are statistically significant lower in tomosynthesis images compared to mammograms ($p\text{-value}<0.0001$); however the coarseness values are strongly correlated for the two modalities ($\rho=0.83$). Contrast is statistically significant higher in tomosynthesis ROIs ($p\text{-value}<0.0001$); the contrast values are also correlated for the two modalities ($\rho=0.64$). Visual examination of the ROIs also supports the fact that texture in tomosynthesis source projections differs from the x-ray mammograms (see Figure 3). The difference in texture can be attributed to differences in the acquisition technique; the tomosynthesis central source projection image is acquired with lower radiation dose, less compression force and without a grid. Less compression force in tomosynthesis changes the superimposition of fibroglandular tissue. The absence of a grid introduces effects from the increased prevalence of x-ray scatter.

3.2 Texture variation in tomosynthesis projection angles

In order to examine the variation of texture features over the angles of tomosynthetic acquisition, we computed skewness, coarseness, and contrast from retroareolar ROIs in all the nine source projection images of each breast for each woman in our dataset (see Figure 7). For each texture feature, we computed the correlation coefficient ρ (20) between the different projection angles and the central source projection, and between consecutive source projection angles. These results are shown in Figures 8-9. Contrast was the most robust feature with respect to angle variation; the correlation coefficients demonstrate that contrast varied little as a function of angle. On the other hand, skewness appears to be the most sensitive feature demonstrating the highest variation in correlation between different angles.

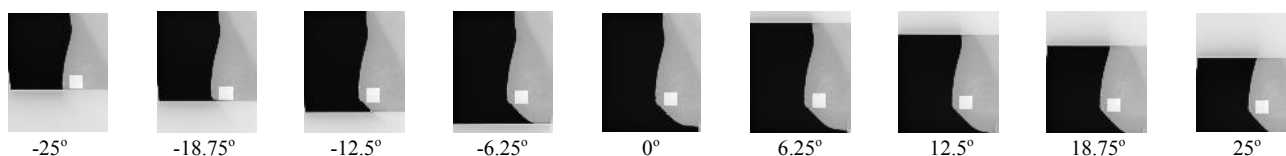


Fig. 7. An example of retroareolar ROIs in all the 9 source projection DBT images.

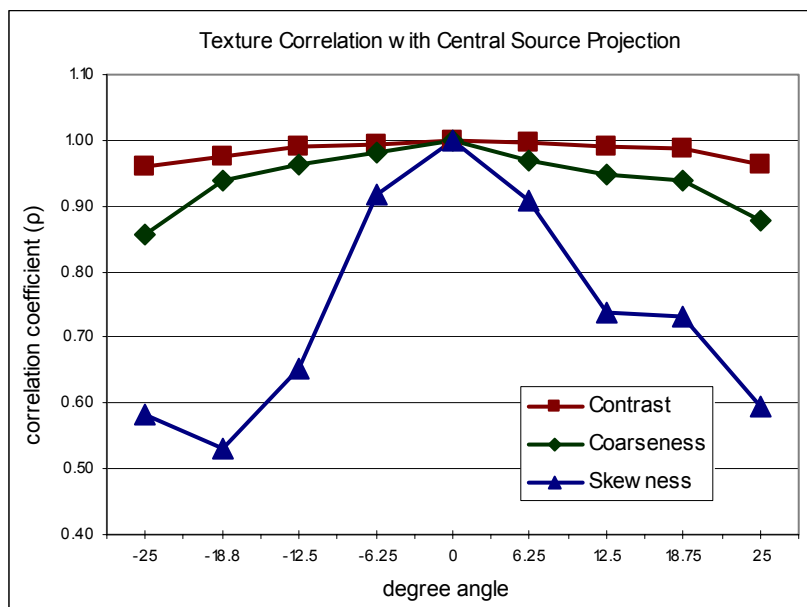


Fig. 8. Correlation of each texture descriptor between each DBT source projection angle and the central source projection

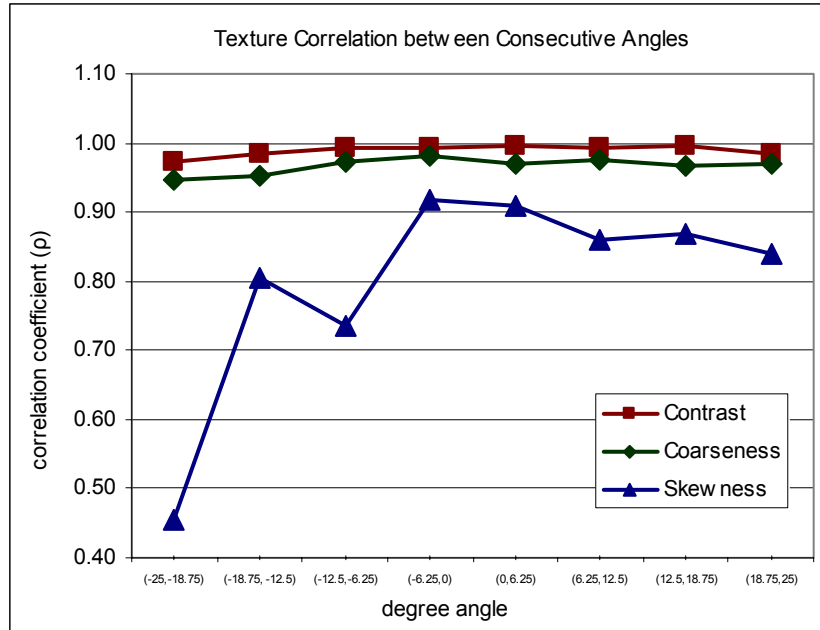


Fig. 9. Correlation of each texture descriptor between every two consecutive DBT source projection angles.

3.3 Effect of scatter on texture

At acute angles, our tomosynthesis acquisition geometry is such that the breast is not fully exposed. As a result, the x-ray collimator is visualized (see Figures 2 and 7). To study the effect of x-ray scatter on texture, we positioned a 256x256 pixel ROI in a central region of the breast at the -25° source projection. The ROI was initially located near the collimator and then translated in one pixel increments over a 512 pixel path. Figure 10 illustrates an example of such an ROI and the corresponding sliding path. In order to investigate the effect of scattered radiation in tomosynthesis texture, we computed skewness, the most sensitive of our texture descriptors in angle variation, for each positioning of the sliding ROIs. The graph in Figure 11 shows the computed skewness averaged over 52 images for each position of the ROI for the tomosynthesis source projection and the same position in the corresponding mammogram; we excluded cases in which visual artifacts or malignancy was present within the sliding path of the ROI in either breast.

As shown in Figure 11, skewness is lower overall in the tomosynthesis images compared to mammograms; the range of the skewness values in the tomosynthesis ROIs is almost double the range of the skewness values in mammograms. These results are different from the ones obtained when comparing skewness in retroareolar ROIs in tomosynthesis CSP and the corresponding mammograms. We attribute this difference to the non-uniform spatial dependence of the scatter near the boundary of the x-ray field.

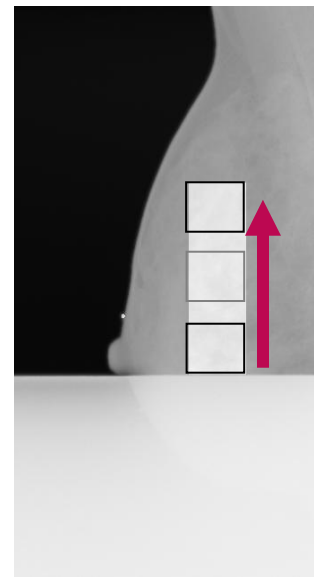


Fig. 10. The initial positioning of the ROI near the collimator and the sliding path of the ROI over 512 pixels.

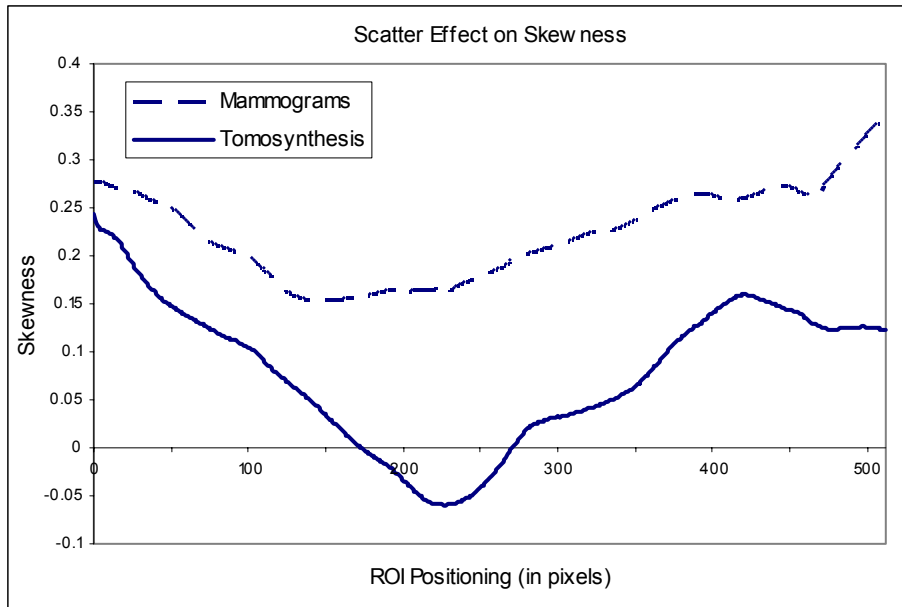


Fig. 11. The computed skewness over all pixel positionings for the tomosynthesis central source projection images and the corresponding mammograms.

3.4 Texture patterns versus Gail and Claus risk

Our ultimate intention is to investigate the relationship between parenchymal texture patterns in tomosynthesis images and breast cancer risk. In this study, our available population of women included women at high risk, women with recently detected malignancies, and follow-up of previous cancer patients. In order to obtain complete results on the correlation between texture features and cancer risk, there is a need to also include a low-risk population in our analysis; we are in the process of obtaining and analyzing such a population. However, as a first step towards investigating this relationship, we examined the patterns of texture versus the calculated Gail risk for each woman in the contralateral tomosynthesis CSP images, compared with the corresponding patterns obtained from the mammograms. Figure 12 shows the coarseness texture patterns versus the Gail risk for the tomosynthesis and mammographic retroareolar ROIs. Although very preliminary, we believe that these results are encouraging. The observed patterns are similar.

4. CONCLUSIONS

In this work we present our initial findings on the relationship between image texture features in tomosynthesis source projection images and corresponding mammograms. The visualized texture in tomosynthesis central source projections differs from x-ray mammograms; however the texture descriptors are correlated for the two imaging modalities. Skewness values in tomosynthesis images did not appear to be statistically significantly different than those in mammograms; the correlation coefficient for the two modalities is $\rho=0.68$. Nevertheless, in terms of their absolute skewness values, tomosynthesis ROIs appeared to be less skewed compared to mammograms ($p\text{-value}<0.001$). Coarseness values are statistically significant lower in tomosynthesis images compared to mammograms ($p\text{-value}<0.0001$); however correlation is strong for the two modalities ($\rho=0.83$). Contrast is statistically significant higher in tomosynthesis ROIs ($p\text{-value}<0.0001$); the contrast values are also correlated for the two modalities ($\rho=0.64$). We attribute these differences in texture to lower radiation dose, smaller compression force and increased x-ray scatter in tomosynthesis. When investigating the variation of texture features as a function of angle, we observed that contrast was the most robust feature with respect to angle variation, while skewness appears to be the most sensitive feature demonstrating the highest variation in the correlation between different angles. Finally, we studied the effect of scatter in tomosynthesis texture and concluded that it has a considerable effect on the computed texture descriptors; this is a factor that should be considered when performing parenchymal pattern analysis in tomosynthesis images.

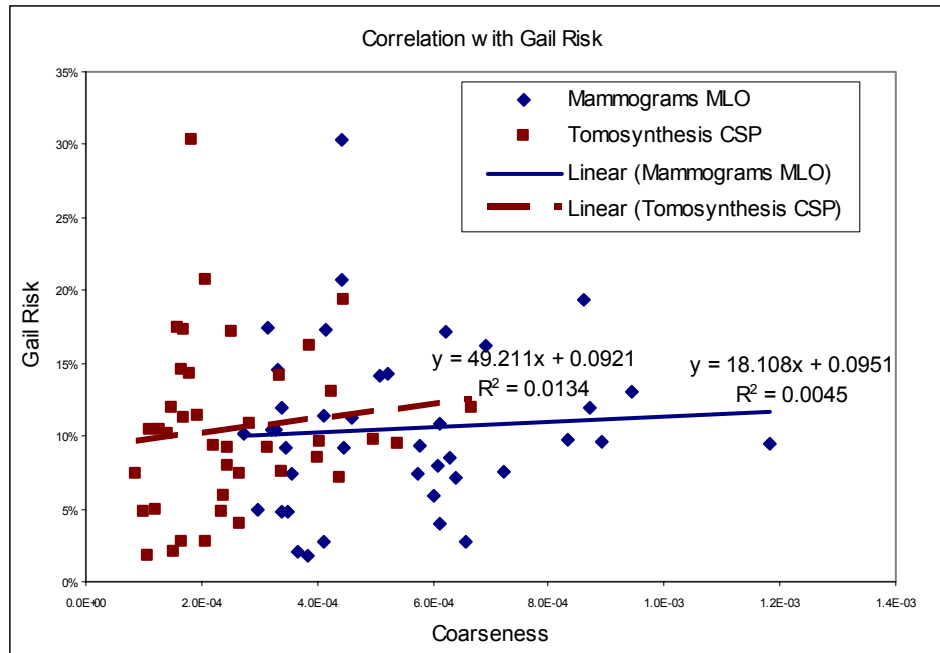


Fig. 12. Scatter-plot with least-square linear regression line for tomosynthesis CSP and mammographic MLO coarseness in the contralateral retroareolar ROIs versus the Gail cancer risk estimates for each woman.

To the best of our knowledge, this is the first report on investigating the differences in texture between tomosynthesis projection images and mammograms. This analysis is independent of reconstruction algorithm (2) and provides a baseline for comparing texture initially with 2D mammograms and ultimately with fully 3D texture assessment from reconstructed tomosynthesis images. We conclude that the acquisition differences between the tomographic projection images and the mammograms do not have a significant negative impact on texture. Our ultimate goal is to examine the correlation between 3D tomosynthesis texture descriptors and breast cancer risk. We believe that texture analysis of 3D breast tomosynthesis images will yield more accurate and precise measures of risk.

ACKNOWLEDGEMENT

This work was funded by the Agfa/RSNA Research Fellowship in Basic Radiologic Sciences FBR0601 and by the Susan G. Komen Breast Cancer Foundation Research Grant BCRT133506. The image acquisition for this study was funded by the National Institutes of Health/National Cancer Institute Program Project Grant P01-CA85484.

REFERENCES

1. Wolfe JN. Risk for breast cancer development determined by mammographic parenchymal pattern. *Cancer (Phila.)* 1976; 37:2486-2492.
2. Wolfe JN. Breast patterns as an index of risk for developing breast cancer. *American Journal of Roentgenology* 1976; 126:1130-1139.
3. Greendale GA, Reboussin BA, Slone S, Wasilaukas C, Pike MC, Ursin G. Postmenopausal hormone therapy and change in mammographic density. *Journal of the National Cancer Institute* 2003; 95:30-37.
4. Byrne C, Schairer C, Wolfe J, et al. Mammographic features and breast cancer risk: effects with time, age, and menopause status. *Journal of the National Cancer Institute* 1995; 87:1622-1629.
5. Li H, Giger ML, Olopade OI, Margolis A, Lan L, Chinander MR. Computerized Texture Analysis of Mammographic Parenchymal Patterns of Digitized Mammograms. *Academic Radiology* 2005; 12:863-873.

6. Huo Z., Giger M.L. WDE, Zhong W., Cumming S., Olopade O.I. Computerized analysis of mammographic parenchymal patterns for breast cancer risk assessment: feature selection. *Medical Physics* 2000; 27:4-12.
7. Li H, Giger ML, Huo Z, et al. Computerized analysis of mammographic parenchymal patterns for assessing breast cancer risk: effect of ROI size and location. *Medical Physics* 2004; 31:549-555.
8. Yaffe MJ, Boyd NF, Byng JW, et al. Breast cancer risk and measured mammographic density. *European Journal of Cancer Prevention* 1998; 7 (suppl 1):S47-S55.
9. Yaffe M, Boyd N. Mammographic breast density and cancer risk: the radiological view. *Gynecological Endocrinology* 2005; 2005:6-11.
10. Niklason LT, Christian BT, Niklason LE, et al. Digital tomosynthesis in breast imaging. *Radiology* 1997; 205:399-406.
11. Rafferty EA. Tomosynthesis: New Weapon in Breast Cancer Fight. *Decisions in Imaging Economics* 2004; 17.
12. Wu T, Moore RH, Rafferty EA, Kopans DA. A comparison of reconstruction algorithms for breast tomosynthesis. *Medical Physics* 2004; 31:2636-2647.
13. Huo Z, Giger ML, Olopade OI, et al. Computerized analysis of digitized mammograms of BRCA1 and BRCA2 gene mutation carriers. *Radiology* 2002; 225:519-526.
14. Gail MH, Brinton LA, Byar DP, et al. Projecting individualized probabilities of developing breast cancer for white females who are being examined annually. *Journal of the National Cancer Institute* 1989; 81:1879-1886.
15. Claus EB, Risch N, Thompson WD. Autosomal dominant inheritance of early-onset breast cancer: Implications for risk prediction. *Cancer (N.Y.)* 1993; 73:643-651.
16. The RSNA Medical Imaging Resource Center (MIRC), <http://www.rsna.org/mirc/> (last accessed February 7, 2007).
17. Caldwell CB, Stapleton SJ, Hodsworth DW, et al. Characterisation of mammographic parenchymal pattern by fractal dimension. *Physics in Medicine and Biology* 1990; 35:235-247.
18. Amadasum M, King R. Textural features corresponding to textural properties. *IEEE Transactions on Systems Man and Cybernetics* 1989; 19:1264-1274.
19. Haralick RM, Shanmugam K, Dinstein I. Textural features for image classification. *IEEE Transactions on Systems, Man and Cybernetics* 1973; 3:610-621.
20. Petrie A, Sabin C. *Medical Statistics at a Glance*: Blackwell Publishing, 2000.